

---

# Self-Predictive Representations for Combinatorial Generalization in Behavioral Cloning

---

Daniel Lawson<sup>1,2,\*</sup> Adriana Hugessen<sup>1,2,\*</sup> Charlotte Cloutier<sup>1,3</sup>

Glen Berseth<sup>1,2,†</sup> Khimya Khetarpal<sup>1,4,†</sup>

<sup>1</sup>Mila <sup>2</sup>Université de Montréal <sup>3</sup>University of Waterloo <sup>4</sup>Google DeepMind

## Abstract

Behavioral cloning (BC) methods trained with supervised learning (SL) are an effective way to learn policies from human demonstrations in domains like robotics. Goal-conditioning these policies enables a single generalist policy to capture diverse behaviors contained within an offline dataset. While goal-conditioned behavior cloning (GCBC) methods can perform well on in-distribution training tasks, they do not necessarily generalize zero-shot to tasks that require conditioning on novel state-goal pairs, i.e. *combinatorial generalization*. In part, this limitation can be attributed to a lack of temporal consistency in the state representation learned by BC; if temporally related states are encoded to similar latent representations, then the out-of-distribution gap for novel state-goal pairs would be reduced. Hence, encouraging this temporal consistency in the representation space should facilitate combinatorial generalization. Successor representations, which encode the distribution of future states visited from the current state, nicely encapsulate this property. However, previous methods for learning successor representations have relied on contrastive samples, temporal-difference (TD) learning, or both. In this work, we propose a simple yet effective representation learning objective, BYOL- $\gamma$  augmented GCBC, which is not only able to theoretically approximate the successor representation in the finite MDP case without contrastive samples or TD learning, but also, results in competitive empirical performance across a suite of challenging tasks requiring combinatorial generalization.

## 1 Introduction

Generalization has been a long-standing goal in machine learning and robotics. Recently, large-scale supervised models for language and vision have demonstrated impressive generalization when trained over vast amounts of data. In the robotics domain, this has motivated the development of large-scale supervised behavior cloning (BC) models trained on offline datasets of diverse demonstrations [17, 24]. However, these models still suffer from a lack of generalization. In particular, while BC methods can perform well on tasks directly observed in the dataset, they often fail to perform zero-shot transfer to tasks requiring novel combinations of in-distribution behavior, known as *combinatorial generalization*. In the robotics domain, where demonstration data is time-intensive and costly to produce, simply scaling the dataset is often not possible. Hence, achieving this type of generalization algorithmically will be critical to unlocking the potential for large-scale supervised policy training.

The property of combinatorial generalization has been previously formalized as the ability to “stitch” [18]. Specifically, stitching refers to the ability of a policy to reach a goal state from a start state when trained on a dataset of trajectories which, provides sufficient coverage of the path to the goal, but which does not contain a single complete trajectory of the path. The lack of stitching observed

\* Co first author. † Equal advising. Project page: <https://self-pred-bc.github.io/>.

Correspondence: {daniel.lawson, adriana.knatchbull-hugessen}@mila.quebec

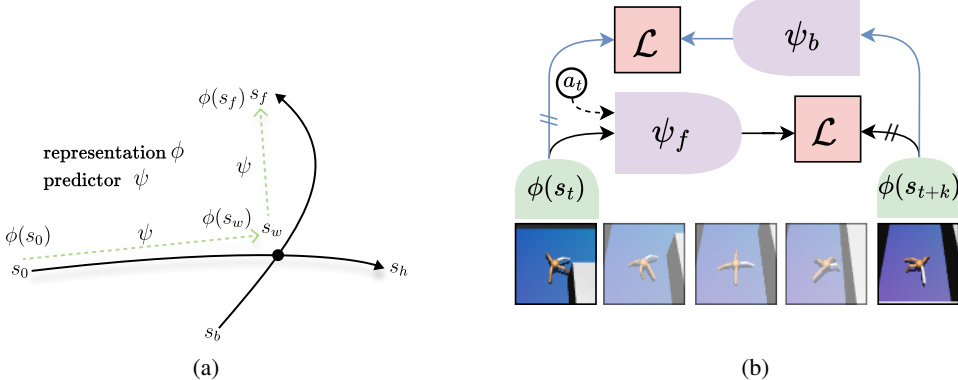


Figure 1: (a) **Self-predictive Representations.** Example training trajectories,  $s_0 \rightarrow s_h$  and  $s_b \rightarrow s_f$ , which intersect at  $w$ . After training on these trajectories, we evaluate on a task like  $s_0 \rightarrow s_f$ , requiring combinatorial generalization. To learn better representations for generalization, a self-predictive representation predicts a future state  $\phi(w)$  from an earlier state  $\phi(e)$  via  $\psi(\phi(e))$ . (b) **Representation learning with BYOL- $\gamma$ .** We predict future state representations  $\phi(s_{t+k})$  via  $\psi_f(\phi(s_t), a)$ , and also predict backwards with  $\psi_b(\phi(s_{t+k}))$ . The target offset is sampled geometrically:  $k \sim \text{geom}(1 - \gamma)$ . Stop-gradients are denoted by  $//$ . We provide more details on the loss  $\mathcal{L}$  in Section 4.2.

in goal-conditioned behavioral cloning (GCBC) and, more generally, supervised learning, can be understood through the inductive biases of the model. By construction, BC methods do not encode the inductive bias that the observed data are generated from a Markov decision process (MDP). In contrast, reinforcement learning (RL) policies that are trained via temporal difference (TD) learning directly utilize the structure of the MDP, and pass information through time using dynamic programming. Offline RL [29] has been proposed as a method for achieving stitching in policies trained on offline datasets. However, these methods are challenging to scale due to the instability of bootstrapping in TD learning when combined with fully offline training. Scaling has been more successful with supervised methods, such as in robotics, where training robot foundation models with BC [17, 24] on large-scale datasets [39, 22] can lead to more general-purpose policies.

Various methods have attempted to imbue GCBC models with the ability to stitch by augmenting the training data using the Markovian assumption [52, 18]. However, these methods ultimately rely on similar training procedures as offline RL or otherwise require a distance metric already aligned with temporal distance in the MDP. Another approach frames stitching as a representation learning problem [36]. In this context, the objective is to learn a latent representation of states that reflects temporal proximity in the underlying MDP to facilitate generalization to unseen state-goal pairs. In particular, Myers et al. [36] train a representation that approximates the successor measure (SM) [2] through contrastive learning (CL) [48] as an auxiliary loss in GCBC, demonstrating enhanced combinatorial generalization. This is a promising step towards achieving combinatorial generalization in GCBC methods. In this work, we expand on this connection between the successor measure and combinatorial generalization, proposing an alternative objective that captures similar properties with a simpler learning procedure and achieves as good or better generalization performance.

In particular, in other domains, like vision, it has been found that contrastive learning can often be substituted with self-predictive representations [19], which have also been found to be useful as auxiliary losses for model-free RL [44]. Adapting the *Bootstrap Your Own Latent* (BYOL) framework [19] to the RL setting, representations can be trained by predicting the latent representation of the next state from the current latent state representation. These BYOL objectives have appealing properties, such as neither relying on negative examples nor reconstruction.

As motivation, we foremost evaluate the BYOL objective as an auxiliary loss for GCBC; however, we find that there exists an empirical and theoretical gap compared to contrastive methods. This leads us to propose a novel objective, **BYOL- $\gamma$** , which removes the gap between self-predictive and contrastive objectives. Concretely, BYOL- $\gamma$  predicts latent representations of states sampled from a  $\gamma$ -discounted future state distribution. While the standard BYOL objective has been shown to learn representations capturing spectral information about the one-step transition dynamics [23], we show that the representations learned by BYOL- $\gamma$  capture spectral information related to the

successor measure. In the finite MDP case, we show that, in fact, BYOL- $\gamma$  approximates the successor representation. Empirically, we demonstrate on the challenging OGBench dataset [40] that BYOL- $\gamma$  augmented GCBC is competitive with contrastive methods in improving combinatorial generalization.

**Key contributions of our work** are as follows:

- We propose BYOL- $\gamma$ , a novel representation learning objective that relates to the successor measure, which we prove in the finite MDP setting.
- Empirically, we demonstrate that such a BYOL objective can be used as auxiliary objective augmenting the capabilities of Behavior Cloning, and we find that BYOL- $\gamma$  obtains competitive results on navigation tasks in OGBench compared to existing methods.
- Qualitatively, we show that the BYOL- $\gamma$  objective learns similar representation structures to CL, encoding temporal distance between states.

## 2 Related Work

**Stitching in Supervised Methods.** Outcome (goals or return)-conditioned behavioral cloning (OCBC) methods [43, 8, 11] provide a simple and scalable alternative to traditional offline RL [29] methods. However, these methods do not properly “stitch” and generalize to unseen outcomes [3, 18]. To reduce this problem, various works have proposed augmenting training data used by BC methods. Some work incorporates methodology from offline RL to label returns or goals for downstream SL [7, 52]. Other work has considered relabeling goals through clustering states [18], which relies on a good distance metric in state-space and is limited to short trajectory stitches. Other work has utilized planning [54] for goal relabeling, or generative models to synthesize new trajectories [31, 28]. Rather than using models to generate data for BC, other work directly evaluates the combinatorial generalization achieved by planning with generative models [32]. In this work, we neither require combining SL with explicit Q-learning, utilize generative models, or perform explicit planning.

**Visual Representation Learning.** Instead of auxiliary representation learning, prior work has considered using pretrained visual representations for BC. Utilizing pretrained BC has been a reliable method to efficiently learn policies and improve generalization [42, 33, 37]. Instead of pretraining representations out-of-domain, such as on large image datasets, DynaMo [9] evaluates pretraining representations in-domain on specific robotics datasets, and then performs a separate BC finetuning stage. However, we focus on representation learning as an auxiliary objective. For enhancing combinatorial generalization, this can be advantageous, as training as an auxiliary task maintains the structure of the representation space, and prevents overfitting the BC objective.

**Representation learning in RL.** Our objective is most closely related to approaches using auxiliary **BYOL objectives in online RL** [16, 44, 38, 49]. These objectives can help with sample-efficiency, such as in challenging, partially observed environments with sparse rewards, or with noisy states. Additionally, self-predictive dynamics models are used in planning and model-based RL [14, 53, 21]. Various works have also characterized the dynamics of BYOL objectives in the RL setting, showing that BYOL objectives capture spectral information about the policy’s transitions [46, 23]. In the offline setting, how well Joint Embedding Predictive Architecture (JEPA) world models generalize when used for explicit planning has been studied [45], however not for combinatorial generalization. Additionally, certain representation structures for value functions, namely quasimetrics [30, 51, 50, 34] can also lead to policies that better generalize to longer horizons [35]. Quantities related to the **Successor Representation** (SR) [10], such as successor features (SF) [1], and the successor measure (SM) [2] have been widely used for generalization and transfer in reinforcement learning [5]. Similarly to BYOL, these objectives have been used for representation learning in RL [26, 13]. While prior BYOL methods either perform 1-step, or relatively short fixed n-step prediction, neither of these choices directly approximate the successor measure. Our setup is most related to temporal representation alignment (TRA) [36], which recently proposed using contrastive learning as an auxiliary objective for BC to improve combinatorial generalization. In this work, we further build on the relationship between the SM and combinatorial generalization, and propose new representation learning objectives which can lead to better performance.

## 3 Background

**Controlled Markov Process.** We consider goal-conditioned decision-making problems, with state space  $\mathcal{S}$ , goals  $g \in \mathcal{G}$ , action space  $\mathcal{A}$ , initial state distribution  $p_0(s)$ , dynamics  $p(s_{t+1} | s_t, a)$ , and with policies  $\pi(a|s, g)$ .

**Successor Representation (SR) and Successor Measure (SM).** In a finite MDP, the *successor representation* (SR) [10] of a policy is:

$$M^\pi(s, s') := \mathbb{E} \left[ \sum_{t \geq 0} \gamma^t \mathbb{1}_{(s_{t+1}=s')} \mid s_0 = s, \pi \right] \quad (1)$$

We use the convention of counting from  $s_{t+1}$ , writing in matrix form  $M^\pi = \sum_{t \geq 0} \gamma^t (P^\pi)^{t+1}$ . The transition matrix transition for policy  $\pi$  is  $P^\pi$ , with  $P_{i,j}^\pi = \sum_a \pi(a|s=i) P_{i,a,j}$ , where  $P_{i,a,j} = p(s_{t+1}=j \mid s_t=i, a)$ . The successor representation also satisfies the bellman equation,  $M^\pi = P^\pi + \gamma P^\pi M^\pi = P^\pi(I - \gamma P^\pi)^{-1}$ . For a fixed policy, the successor representation describes a type of temporal distance between states. The *successor measure* (SM) [2] extends SR to continuous spaces  $S$ :  $M^\pi(s, X) := \sum_{t \geq 0} \gamma^t P(s_{t+1} \in X \mid s) \forall X \subset S$ . We also define the *normalized* successor representation, or measure  $\tilde{M}^\pi = (1 - \gamma) M^\pi$ . In the finite case, the normalized successor representation  $\tilde{M}^\pi$  has rows that sum to one like transitions  $P^\pi$ . Another quantity *successor features* (SF) [1] are the expected discounted sum of future features  $\phi(s) \in \mathbb{R}^d$ :  $\psi^\pi(s) = \mathbb{E} \left[ \sum_{t \geq 0} \gamma^t \phi(s_{t+1}) \mid s_0 = s, \pi \right]$ . We can relate SFs to the SM with  $\psi^\pi(s) = \int_{s'} M^\pi(s, s') \phi(s')$ . Each of these quantities can also be defined with conditioning on the first action and then following the policy, e.g.  $M^\pi(s, a, s')$ .

### 3.1 Representation Learning

We begin with two representation learning methods that approximate the density of the SM.

**Forward-Backward.** We consider a simplified version of the Forward-Backward loss that approximates the successor measure for a fixed policy  $\pi$ , discussed by Touati et al. [47].

$$\min_{\phi, \psi} \mathbb{E}_{\substack{s_t \sim p(s), s' \sim p(s) \\ s_{t+1} \sim p^\pi(s_{t+1} \mid s_t)}} [(\psi(s_t)^T \phi(s') - \gamma \bar{\psi}(s_{t+1})^T \bar{\phi}(s'))^2] - 2 \mathbb{E}_{\substack{s_t \sim p(s) \\ s_{t+1} \sim p^\pi(s_{t+1} \mid s_t)}} [\psi(s_t)^T \phi(s_{t+1})] \quad (2)$$

FB learns an approximation of the successor measure with factorization  $M^\pi(s, s_+) \approx \psi(s_t) \phi(s_+) p(s_+)$  using TD learning. Given transitions  $(s_t, s_{t+1})$  sampled by a policy  $\pi$ , the second term relates to fitting  $M^\pi(s_t, s_{t+1})$ . Given an independently sampled state  $s'$ , the first term bootstraps an estimate of  $M^\pi(s_t, s')$  from  $M^\pi(s_{t+1}, s')$ , where  $\bar{\phi}, \bar{\psi}$  denote stop-gradient operations.

**Contrastive Learning.** Temporal contrastive learning used in MDPs [12] is related to a Monte Carlo (MC) approximation of the (discounted) successor measure. This can be implemented with a InfoNCE [48] loss that maximizes the similarity of a positive pair between a state  $s_t$  and a future state from the same trajectory  $s_+$ , and minimizing the similarity of  $s_t$  and random states  $s_-$ :

$$\max_{\phi, \psi} \mathbb{E}_{\substack{s_t \sim p(s) \\ k \sim \text{geom}(1-\gamma) \\ s_+ = s_{t+k}, s_-^{2:N} \sim p(s)}} \left[ \log \frac{e^{f(\psi(s_t), \phi(s_+))}}{\sum_{i=2}^N e^{f(\psi(s_t), \phi(s_-^i))}} \right] \quad (3)$$

A common choice for the energy function  $f$  is the inner product  $f(\psi(s) \phi(s_+)) = \psi(s)^T \phi(s_+)$ . A key aspect to note is that the positive sample  $s_+$  comes from an MC sample from  $s_+ \sim M^\pi(s_t, s_+)$ . The optimal solution to (3) gives  $\tilde{M}^\pi(s, s_+) \approx C \exp(\psi(s_t)^T \phi(s_+)) \cdot p(s)$ . However in-practice, we only have dataset of MC samples from  $\pi$ , i.e. fixed-length trajectories, which means we do not actually estimate the SM of  $\pi$ . In Appendix C, we further elaborate on the relationship between the FB loss, and CL. Particularly, in the limit, an n-step version of FB is related to CL.

**BYOL.** We now look at an objective that captures information about single-step transition instead of the successor measure. In the context of RL, self-predictive models jointly learn a latent space and a dynamics model through predicting future latent representations. Self-predictive models rely on latent bootstrapped targets (BYOL) [19], avoiding reconstruction (generative models), or negative samples (contrastive learning). Self-predictive models are also a type of joint-embedding predictive architectures (JEPAs) [27, 15].

Given an encoder which produces a representation  $z_t = \phi(s_t)$ , and dynamics  $\psi(z_{t+1} \mid z_t)$  for a fixed policy  $\pi$ , we minimize the difference between our prediction and target representation in latent-space:

$$\min_{\phi, \psi} \mathbb{E}_{s_t \sim p(s), s_{t+1} \sim p^\pi(s_{t+1} \mid s_t)} [f(\psi(\phi(s_t)), \bar{\phi}(s_{t+1}))] \quad (4)$$

Where  $f$  is a convex function such as the squared  $l_2$  norm, and  $\bar{\phi}$  refers to an EMA target, or stop-gradient. Variants of this BYOL objective have been widely used to learn state abstractions, and work as an auxiliary loss when approximating the value function in deep RL [16, 44, 38]. In the finite MDP, this objective captures spectral information about the policy’s transition matrix  $P^\pi$  [46, 23] which we discuss in Appendix D.1.

### 3.2 Combinatorial Generalization from Offline Data

We now shift focus on how we can learn policies from offline data using behavioral cloning, and then introduce a combinatorial generalization gap that arises in this setting.

We consider a **dataset**  $\mathcal{D} = \{(s_0^i, a_0^i, \dots, s_T^i, a_T^i)\}_{i=1}^N$ , composed of trajectories generated by a set of unknown policies  $\{\beta_j(a|s)\}$ . **Goal Conditioned Behavioral Cloning (GCBC)** trains a policy with maximum likelihood to reproduce the behaviors from the dataset. After sampling a current state, a goal is sampled as a future state from the same trajectory:

$$\max_{\pi} \mathcal{L}_{\text{BC}}(\pi) = \max_{\pi} \mathbb{E}_{\substack{\beta_j \sim p(\beta_j), s \sim p(s|\beta_j) \\ a \sim \beta_j(a|s), s_+ \sim M^{\beta_j}(s, s_+)}} [\log \pi(a|s, g = s_+)] \quad (5)$$

**Generalization gap.** While this policy can perform well in-distribution, the behavior cloning policy struggles to generalize to reach goals from states that are not in matching training trajectories. We now review a more formal definition of this type of generalization gap.

We consider Lemma 3.1 from Ghugare et al. [18], which says there exists a single Markovian policy  $\beta(a|s)$  that has the same occupancy as the mixture of  $j$  policies:

$$M^\beta(s) = \mathbb{E}_{p(\beta_j)} [M^{\beta_j}(s)] \quad (6)$$

This policy also has construction:  $\beta(a|s) := \sum_j \beta_j(a|s)p(\beta_j|s)$ , where  $p(\beta_j|s)$  is the distribution over policies in  $s$  as reflected by the dataset.

Using the successor measure of the individual policies, and the mixture policy, we can quantify a gap between accomplishing out-of-distribution tasks versus in-distribution training tasks [18]:

$$\underbrace{\mathbb{E}_{\substack{s_0 \sim M^\beta(s_0) \\ s_g \sim M^\beta(s_0, s_g)}} [u^\pi(s_0, s_g)]}_{\text{tasks requiring combinatorial generalization}} - \underbrace{\mathbb{E}_{\substack{\beta_j \sim p(\beta_j), s_0 \sim M^{\beta_j}(s_0) \\ s_g \sim M^{\beta_j}(s_0, s_g)}} [u^\pi(s_0, s_g)]}_{\text{in-distribution training tasks}} \quad (7)$$

Here,  $u$  is a performance metric of the policy  $\pi$  such as the success rate to reach  $s_g$  from  $s_0$ . As we perform well on in-distribution tasks due to a correspondence to Equation (5), the BC policy has no guarantees for the first term. This is because after sampling a state, the goal is sampled from the successor measure of the mixture policy.

## 4 Closing the Generalization Gap with Representations

In this section, we aim to close the aforementioned generalization gap. We consider a policy trained with the BC objective  $\pi$  to be made more robust to the tasks requiring combinatorial generalization through representation learning. We begin with a setup similar to Equation (7), but with a shared initial state  $s_0$  for both the in-distribution and out-of-distribution task. For the in-distribution task, we sample a goal as before, labeled as  $s_w$ . However, for the out-of-distribution task, we sample a goal  $s_f$  to be a state that can be reached by the mixture policy  $\beta$  after  $s_w$ . (8):

$$\mathbb{E}_{\substack{\beta_j \sim p(\beta_j), s_0 \sim M^{\beta_j}(s) \\ s_w \sim M^{\beta_j}(s_0, s_w)}} \left[ \underbrace{\mathbb{E}_{s_f \sim M^\beta(s_w, s_f)} [u^\pi(s_0, s_f)]}_{\text{extended task requiring generalization}} - \underbrace{u^\pi(s_0, s_w)}_{\text{in-distribution task}} \right] \quad (8)$$

$$= \mathbb{E}_{\substack{\beta_j \sim p(\beta_j), s_0 \sim M^{\beta_j}(s) \\ s_w \sim M^{\beta_j}(s_0, s_w)}} \left[ \underbrace{\mathbb{E}_{s_f \sim M^\beta(s_w, s_f)} [u^\pi(s_0, \phi(s_f))]}_{\text{want invariance with respect to future goals through } \phi} - u^\pi(s_0, \phi(s_w)) \right] \quad (9)$$

Then, in Equation (9) we add a goal representation  $\phi$  that processes the goal before going to policy  $\pi$ . Intuitively, a policy could achieve the out-of-distribution task by first going from  $s_0$  to  $s_w$  (in-distribution), and then completing the remaining task  $s_w$  to  $s_f$ . In essence, we want that when

conditioning on  $\phi(s_f)$ , the policy should first go to  $s_w$ , which can be achieved by learning  $\phi$ , where  $\phi(s_w)$  is similar to  $\phi(s_f)$  [36]. More formally, for  $s_f \sim M^\beta(s_w, s_f)$  we want an invariance  $\phi(s_f) \approx \phi(s_w)$ .

From this observation, we can understand that approximating the successor measure of the mixture policy  $\beta$ , when parameterized by  $\phi$ , will build the desired representation. One choice for the representation learning objective can be the FB algorithm, which obtains a factorization  $M^\beta(s, s_+) \approx \psi(s_t)\phi(s_+)p(s_+)$  [47]. FB utilizes TD-learning to learn the same representations given transitions  $(s_t, s_{t+1})$ , regardless of how these transitions are divided between trajectories. However, FB may not scale as well to large datasets and high-dimensional state spaces. This may lead us to prefer an MC approximation of the SM, using CL. A key point here is that we do not have MC samples from  $\beta$ , only the individual policies  $\beta_j$ , so CL does not directly approximate  $M^\beta$ . However, in practice, CL can still build a representation space with a compositional structure [36], and may be a more scalable option than FB.

#### 4.1 BYOL- $\gamma$ : Connecting self-predictive objectives to the successor representation

To build representations that lead to generalization, we propose a predictive objective, relying on neither TD learning nor negative samples. Specifically, we propose BYOL- $\gamma$  which allows us to use the BYOL framework to capture information related to *successor representations* and its generalizations. Given a state  $s_t$ , a BYOL objective would normally sample a prediction target from a one-step transition  $s_{t+1}$  as in Equation (4). However, we make a modification to predict empirical samples from the normalized successor measure:

$$\mathcal{L}_{\text{BYOL-}\gamma}(\phi, \psi) = \mathbb{E}_{\substack{s_t \sim p(s), k \sim \text{geom}(1-\gamma) \\ s_{t+k} \sim p^\pi(s_{t+k}|s_t)}} [f(\psi(\phi(s_t)), \bar{\phi}(s_{t+k}))] \quad (10)$$

Where  $f$  refers to an energy function,  $\phi$  refers to the encoder, and  $\psi$  the predictor. With  $\gamma = 0$ , we have  $s_{t+k} = s_{t+1}$  corresponding to an approximation of the one-step transitions, recovering the base BYOL objective. Figure 1b depicts our overall representation learning objective. We can view this objective as iteratively minimizing an upper-bound on the error between  $\psi(\phi(s))$  and the true successor features of the policy  $\psi^\pi$  with changing basis features  $\bar{\phi}$ . With convex  $f$ , by Jensen's inequality we have:

$$\mathcal{L}_{\text{BYOL-}\gamma}(\phi, \psi) = \mathbb{E}_{s_t \sim p(s), s_+ \sim \tilde{M}^\pi(s_t, s_+)} [f(\psi(\phi(s_t)), \bar{\phi}(s_+))] \quad (11)$$

$$\geq \mathbb{E}_{s_t \sim p(s)}, [f(\psi(\phi(s_t))) \mathbb{E}_{s_+ \sim \tilde{M}^\pi(s_t, s_+)} \bar{\phi}(s_+)] \quad (12)$$

$$= \mathbb{E}_{s_t \sim p(s)} [f(\psi(\phi(s_t)), (1-\gamma)\psi_\phi^\pi(s_t))] \quad (13)$$

Specifically, in the finite MDP, we can precisely describe the relationship of our objective to the SR with the following result:

**Theorem 4.1.** *Given a finite MDP with linear representations  $\Phi \in \mathbb{R}^{|\mathcal{S}| \times d}$ , and predictor  $\Psi \in \mathbb{R}^{d \times d}$ , under assumptions of orthogonal initialization for  $\Phi$  (Ass. D.1), a uniform initial state distribution  $p_0(s)$  (Ass. D.2), and symmetric transition dynamics (Ass. D.3), minimizing the self-predictive learning objective  $\mathcal{L}_{\text{BYOL-}\gamma}(\phi, \psi)$  approximates a matrix decomposition of the successor representation  $\tilde{M}^\pi \approx \Phi \Psi \Phi^T$ , corresponding to successor features  $(1-\gamma)\Psi^\pi \approx \Psi \Phi$ .*

Proof is in Appendix D.2, where we show that existing theory [23] also translates to the proposed BYOL- $\gamma$  objective. Finally, we can see the relation between this objective and CL (3), with the most striking difference being the removal of the denominator involving negative samples. Surprisingly, we reveal that this simplified system still captures similar information and also can lead to empirical generalization in Section 5.1.

**BYOL- $\gamma$  Variants.** We discuss a few variants on our base objective, namely, we find it beneficial to consider **bidirectional prediction** [20, 46] where we add an additional backwards predictor  $\psi_b$  which predicts a past representation from the future:

$$\mathcal{L}_{\text{BYOL-}\gamma}(\phi, \psi) = \mathbb{E}_{s_t \sim p(s), s_+ \sim \tilde{M}^\pi(s_t, s_+)} [f(\psi_f(\phi(s_t)), \bar{\phi}(s_+)) + f(\bar{\phi}(s_t), \psi_b(\phi(s_+)))] \quad (14)$$

We utilize an **action-conditioned** variant of the forward predictor  $\psi_f(\phi(s_t), a_t)$ , which can be interpreted as a temporally extended latent dynamics model, or capturing information about  $\tilde{M}^\pi(s, a, s_+)$ .

## 4.2 Training a policy with auxiliary BYOL- $\gamma$

We consider BYOL- $\gamma$  as an auxiliary loss for a BC policy  $\pi_\Theta(a|s, g)$ ,  $\Theta = (\theta, \phi, \psi)$ , to better address generalization of a policy. The parameters of the encoder and predictor correspond to  $\phi, \psi$ , and  $\theta$  includes additional parameters such as a policy head which transforms representations to actions. With this policy, we train with the objective:

$$\begin{aligned} \mathcal{L}_{\text{BC}}(\Theta) + \alpha \mathcal{L}_{\text{BYOL-}\gamma}(\phi, \psi) \\ = \mathbb{E}_{(s_t, a_t, s_+) \sim \mathcal{D}} [-\log \pi_\Theta(a|\phi(s), g = \phi(s_+))] \\ + \alpha \mathbb{E}_{(s_t, a_t, s_+) \sim \mathcal{D}} [f(\psi_f(\phi(s_t), a_t), \bar{\phi}(s_+)) + f(\bar{\phi}(s_t), \psi_b(\phi(s_+)))] \end{aligned} \quad (15)$$

For  $f$ , we choose a cross-entropy loss between the (softmax) normalized representations of the prediction and the target, similar to DINO [4]:  $f_{\text{CE}}(a, b) = \text{softmax}(b) \cdot \log \text{softmax}(a)$ . We also find a normalized  $l_2$  loss,  $f_{l_2} = \|\frac{a}{\|a\|} - \frac{b}{\|b\|}\|_2^2$ , commonly used in BYOL setups [19, 44] also works, which we ablate in Section 5.4. We describe additional training details in Appendix A.1.

## 5 Experiments

We have shown the theoretical basis for BYOL- $\gamma$  as an appropriate choice of representation learning objective for combinatorial generalization. Next, we demonstrate its performance empirically. Namely, we compare our proposed method BYOL- $\gamma$  to alternative representation learning methods. We compare representation learning algorithms across three axes: (1) First, we compare qualitatively whether the representations appear to capture temporal relationships (2) Second, we assess representations quantitatively by measuring zero-shot generalization performance on unseen tasks that require combinatorial generalization (3) Third, we assess generalization performance over an increasing generalization horizon. Finally, we perform ablations on the various components of our proposed method to demonstrate the relative importance of each algorithmic choice.

**Environments** We empirically evaluate how well our approach can help with combinatorial generalization on offline goal-reaching tasks on OGBench [40], which contains both navigation and manipulation tasks, across both low-dimensional and visual observations. We focus on navigation environments, where OGBench provides `stitch` datasets, that assess combinatorial generalization by training on trajectories that span at most 4 maze cells, while evaluating on tasks that are longer, requiring combining information from multiple smaller trajectories.

**Baselines** We benchmark against non-hierarchical methods, that perform end-to-end control from state to low-level actions (e.g. joint-control). In addition to BYOL- $\gamma$  used as an auxiliary loss for BC, we evaluate several baselines: **GCBC** is the standard behavioral cloning baseline, which we aim to improve upon with representation learning objectives. **Offline RL** from OGBench, including implicit {V,Q}-learning (**IVL**, **IQL**) [25], Quasimetric RL (**QRL**) [51], and Contrastive RL (**CRL**) [12]. **BYOL** is a minimal version of our BYOL- $\gamma$  setup with 1-step prediction ( $\gamma = 0$ ), only forwards prediction ( $\psi_f$ ) without action-conditioning ( $\psi_f(\phi(s_t))$ ), and loss  $f_{l_2}$ . **TRA** [36] is an auxiliary representation objective using contrastive learning related to an MC approximation of the successor measure **FB**, an on-policy version of forward-backward representation described in Equation (2) used as an auxiliary objective, and is related to TD approximation of the successor measure.

**Experimental Setup** We match the training details of OGBench, and consider a similar representation learning setup to TRA. For TRA and FB, we utilize a similar setup described in Section 4.2. We found it was beneficial to add action conditioning to FB, but did not see an overall improvement for TRA, so we use the original setup without action-conditioning. We provide a full comparison for action-conditioning in Appendix B.1. We note that when we perform action-conditioning, we change the representation of the policy from  $\pi(\phi(s), \psi(g))$  to  $\pi(\phi(s), \phi(g))$ . In Table 1, we utilize superscript  $a$  to denote methods with action-conditioning. Notably, we find that the weight of the auxiliary representation learning objectives ( $\alpha$ ) can be sensitive to both the embodiment, and size of environment (medium vs large). For each method, we perform a hyperparameter sweep over 4  $\alpha$  values, and report the best result for each environment in Table 1. We hold other hyperparameters constant across experiments, except with variation between non-visual and visual environments noted in Appendix A.

## 5.1 Qualitative analysis of representations

In Figure 2, we display a qualitative analysis of the representations. We visualize the similarity between the future prediction  $\psi$  for each state to  $\phi(g)$  for a fixed goal  $g$ . We can see that **BYOL**- $\gamma$  seems to learn a representation that encodes reachability between states, and has a similar structure to **FB**, which is known to approximate the successor measure. **TRA** and base **BYOL** seem to both capture similar structure and learn a less well-defined latent space. However, **BYOL**- $\gamma$  and **FB** have more distinct similarity, and have visible “paths” of similar states. **BYOL**- $\gamma$  also appears to capture the most similarity among more distant pairs of states. Compared to **TRA**, our hypothesis here is that we have more optimistic similarity between distant states due to the lack of a negative term in the loss, which pushes representations apart.

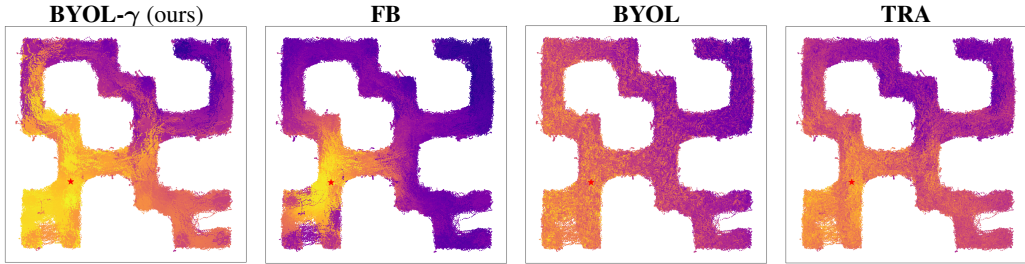


Figure 2: **Visualization of the Learned Representation:** depicts the similarity between the prediction of the current state representation to the goal representation. For **BYOL**- $\gamma$  and **FB**, we visualize the cosine similarity between  $\psi(\phi(s, a)), \phi(g) \forall s \in D$  for a fixed goal  $g$  which is indicated by the star marked in red. For **TRA**, we compare  $\psi(s), \phi(g)$ . **BYOL**- $\gamma$  captures similar temporal relationships as the baseline methods.

## 5.2 Zero-shot performance on combinatorial generalization tasks

In Table 1, we provide the performance results across all methods. Overall, our proposed method **BYOL**- $\gamma$ , shows improved performance vs. **GCBC** across most environments, and is either competitive with or outperforms **FB** and **TRA**. Importantly, we find that a minimal **BYOL** setup does not confer significant benefit over the base **GCBC** except in non-visual **antmaze** environments. Generally, auxiliary representation learning with **GCBC** outperforms existing offline RL methods.

Within the auxillary loss methods, we find that **FB** and **BYOL**- $\gamma$  tend to outperform **TRA** on most environments. While we find that **FB** outperforms **BYOL**- $\gamma$  on environments with smaller state spaces (**antmaze**-{medium, large}), we find that **BYOL**- $\gamma$ ’s simpler training procedure is beneficial in environments with larger state spaces (**humanoidmaze**-{medium, large}, **visual-antmaze**-medium and **visual-scene**-play).

Dataset	BYOL- $\gamma$ <sup>a</sup>	BYOL	TRA	FB <sup>a</sup>	GCBC	GCIVL	GCIQL	QRL	CRL
antmaze-medium-stitch	58 $\pm$ 5	59 $\pm$ 4	54 $\pm$ 6	<b>64 <math>\pm</math> 6</b>	45 $\pm$ 11	44 $\pm$ 6	29 $\pm$ 6	59 $\pm$ 7	53 $\pm$ 6
antmaze-large-stitch	19 $\pm$ 7	17 $\pm$ 6	11 $\pm$ 8	<b>23 <math>\pm</math> 4</b>	3 $\pm$ 3	18 $\pm$ 2	7 $\pm$ 2	18 $\pm$ 2	11 $\pm$ 2
humanoidmaze-medium-stitch	<b>51 <math>\pm</math> 6</b>	23 $\pm$ 3	45 $\pm$ 8	42 $\pm$ 4	29 $\pm$ 5	12 $\pm$ 2	12 $\pm$ 3	18 $\pm$ 2	36 $\pm$ 2
humanoidmaze-large-stitch	<b>13 <math>\pm</math> 3</b>	3 $\pm$ 1	5 $\pm$ 4	11 $\pm$ 3	6 $\pm$ 3	1 $\pm$ 1	0 $\pm$ 0	3 $\pm$ 1	4 $\pm$ 1
antsoccer-arena-stitch	<b>25 <math>\pm</math> 5</b>	12 $\pm$ 7	14 $\pm$ 4	22 $\pm$ 10	<b>24 <math>\pm</math> 8</b>	21 $\pm$ 3	2 $\pm$ 0	1 $\pm$ 1	1 $\pm$ 0
visual-antmaze-medium-stitch	<b>68 <math>\pm</math> 4</b>	57 $\pm$ 8	52 $\pm$ 3	49 $\pm$ 2	<b>67 <math>\pm</math> 4</b>	6 $\pm$ 2	2 $\pm$ 0	0 $\pm$ 0	69 $\pm$ 2
visual-antmaze-large-stitch	26 $\pm$ 5	26 $\pm$ 5	17 $\pm$ 1	<b>29 <math>\pm</math> 2</b>	24 $\pm$ 3	1 $\pm$ 1	0 $\pm$ 0	1 $\pm$ 1	11 $\pm$ 3
visual-scene-play	<b>17 <math>\pm</math> 1</b>	13 $\pm$ 3	<b>16 <math>\pm</math> 3</b>	14 $\pm$ 1	12 $\pm$ 2	25 $\pm$ 3	12 $\pm$ 2	10 $\pm$ 1	11 $\pm$ 2
average	<b>35</b>	26	27	32	26	16	8	14	25

Table 1: **OGBench:** We find that **BYOL**- $\gamma$  performs better overall compared to prior methods. We report mean and standard deviation over 10 training seeds in non-visual environments, and 4 seeds in visual environments. We match the OGBench evaluation setup of 5 evaluation (state,goal) tasks, and 50 episodes per task. The success rate is then averaged over the last 3 checkpoints. We color the best non-RL method, and bold values within 95% of its value in the same row. We use superscript  $a$  to denote methods utilizing action-conditioning.

Interestingly, in **visual-antmaze** **TRA** and **FB** actually seem to hurt performance in comparison to base **GCBC**. On the other hand, with **BYOL**- $\gamma$  we see no performance degradation over **GCBC** on the visual environments, a considerable improvement over other methods.

Dataset	BYOL- $\gamma^a$	$-\alpha$	$f_{l_2}$	$-\psi_b$	$\gamma = 0$
antmaze-medium-stitch	$61 \pm 6$	$63 \pm 9$	$56 \pm 4$	<b><math>67 \pm 2</math></b>	$59 \pm 5$
antmaze-large-stitch	$21 \pm 5$	<b><math>27 \pm 7</math></b>	$24 \pm 6$	$19 \pm 7$	$8 \pm 4$
humanoidmaze-medium-stitch	<b><math>54 \pm 5</math></b>	$48 \pm 5$	$49 \pm 6$	<b><math>52 \pm 5</math></b>	$18 \pm 2$
humanoidmaze-large-stitch	$14 \pm 2$	$12 \pm 6$	<b><math>15 \pm 7</math></b>	$13 \pm 2$	$3 \pm 1$
antsoccer-arena-stitch	$21 \pm 4$	$20 \pm 5$	$11 \pm 5$	<b><math>27 \pm 7</math></b>	<b><math>25 \pm 7</math></b>
visual-antmaze-medium-stitch	<b><math>68 \pm 4</math></b>	<b><math>65 \pm 3</math></b>	$63 \pm 5$	$61 \pm 4$	$54 \pm 9$
visual-antmaze-large-stitch	$26 \pm 5$	$25 \pm 8$	<b><math>27 \pm 7</math></b>	<b><math>28 \pm 2</math></b>	<b><math>28 \pm 1</math></b>
average	33	33	31	33	24

Table 2: **BYOL- $\gamma$  ablations.** We ablate components of our representation learning objective. For each ablation, we perform a hyperparameter sweep over  $\alpha$ , and report the best result per-environment. For all environments, we report results over 4 seeds (for **BYOL- $\gamma$** , we use the first 4 of the 10 reported in Table 1). We color the best method, and bold values within 95% of its value in the same row.

### 5.3 Evaluating generalization with increasing horizon

We conduct experiments to understand how success rate changes as an agent has to reach more challenging goals further away from its starting position. For each maze environment, we consider the same base 5 evaluation tasks used in Table 1, but construct intermediate waypoints along the shortest path to the final goal determined by Breadth First Search. We also include an additional maze environment, giant on which all methods have zero success rates to reach distant goals. This gives a more holistic view on an agent’s performance.

We display results in Figure 3 and Appendix E, where we can see how performance drops off for all methods after a generalization threshold denoted by the red bar. While all methods cannot fully reach distant goals on giant, we see that **BYOL- $\gamma$**  has the slowest drop-off in performance. We note that this is a challenging task, that requires stitching up to approximately 8 different trajectories.

### 5.4 Components affecting generalization for representation learning

We ablate key components of the **BYOL- $\gamma$**  objective in Table 2. This includes removing action conditioning for forward predictor  $\psi_f$  ( $-\alpha$ ), swapping the loss from cross-entropy to normalized squared  $l_2$  norm ( $f_{l_2}$ ), removing backwards predictor  $\psi_b$ , and predicting the representation of the adjacent state ( $\gamma = 0$ ). Both removing action-conditioning, and backwards prediction overall lead to similar results, but variability per-environment. For  $f_{l_2}$ , we obtain slightly worse average performance, and for  $\gamma = 0$ , we see the largest drop-off, especially on humanoidmaze environments.

## 6 Discussion

**Limitations.** While we demonstrate that **BYOL- $\gamma$**  and other representation learning objectives offer a promising recipe for obtaining combinatorial generalization, we find that there still exists a generalization gap, especially on challenging navigation environments e.g. giant. We find a less significant improvement over BC on visual environments, which may motivate additional investigation. Additionally, we may anticipate more benefit from representation learning when applied to larger visual datasets, which has been fruitful in other domains.

**Conclusion.** In this work, we provide a stronger understanding of the relationship between quantities related to successor representations and the generalization of policies trained with behavioral cloning. We propose a new self-predictive representation learning objective, **BYOL- $\gamma$** , and show that it captures information related to the successor measure, resulting in a competitive choice of an auxiliary loss for better generalization. We demonstrate that augmenting behavior cloning with meaningful representations results in new capabilities such as improved combinatorial generalization, especially in larger and more complex environments.

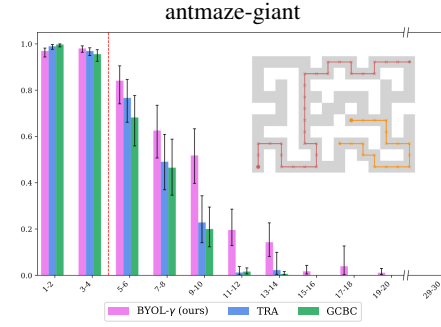


Figure 3: **Evaluating Generalization with Increasing Horizons:** shows that **BYOL- $\gamma$**  not only performs well on goals in the near horizon, but also, generalizes well to goals that requiring stitching occurring after the red bar ( $> 4$ ).

## 7 Acknowledgments

The authors thank Zhaohan Daniel Guo, Faisal Mohamed, and Özgür Aslan for feedback on drafts of the work.

We want to acknowledge funding support from Natural Sciences and Engineering Research Council of Canada, Samsung AI Lab, Google Research, Fonds de recherche du Québec and The Canadian Institute for Advanced Research (CIFAR) and compute support from Digital Research Alliance of Canada, Mila IDT, and NVidia.

## References

- [1] André Barreto, Will Dabney, Rémi Munos, Jonathan J Hunt, Tom Schaul, Hado P van Hasselt, and David Silver. Successor features for transfer in reinforcement learning. *Advances in neural information processing systems*, 30, 2017. URL <https://arxiv.org/abs/1606.05312>. 2, 3
- [2] Léonard Blier, Corentin Tallec, and Yann Ollivier. Learning successor states and goal-dependent values: A mathematical viewpoint, 2021. URL <https://arxiv.org/abs/2101.07123>. 1, 2, 3, C
- [3] David Brandfonbrener, Alberto Bietti, Jacob Buckman, Romain Laroche, and Joan Bruna. When does return-conditioned supervised learning work for offline reinforcement learning? In Alice H. Oh, Alekh Agarwal, Danielle Belgrave, and Kyunghyun Cho, editors, *Advances in Neural Information Processing Systems*, 2022. URL <https://openreview.net/forum?id=XByg4kotW5>. 2
- [4] Mathilde Caron, Hugo Touvron, Ishan Misra, Hervé Jegou, Julien Mairal, Piotr Bojanowski, and Armand Joulin. Emerging properties in self-supervised vision transformers. In *2021 IEEE/CVF International Conference on Computer Vision (ICCV)*, pages 9630–9640, 2021. doi: 10.1109/ICCV48922.2021.00951. 4.2
- [5] Wilka Carvalho, Momchil S. Tomov, William de Cothi, Caswell Barry, and Samuel J. Gershman. Predictive representations: Building blocks of intelligence. *Neural Computation*, 36(11):2225–2298, 10 2024. ISSN 0899-7667. doi: 10.1162/neco\_a\_01705. URL [https://doi.org/10.1162/neco\\_a\\_01705](https://doi.org/10.1162/neco_a_01705). 2
- [6] Yash Chandak, Shantanu Thakoor, Zhaohan Daniel Guo, Yunhao Tang, Remi Munos, Will Dabney, and Diana L Borsa. Representations and exploration for deep reinforcement learning using singular value decomposition. In *International Conference on Machine Learning*, pages 4009–4034. PMLR, 2023. URL <https://arxiv.org/abs/2305.00654>. D.1
- [7] Ian Char, Viraj Mehta, Adam Villaflor, John M. Dolan, and Jeff Schneider. Bats: Best action trajectory stitching, 2022. URL <https://arxiv.org/abs/2204.12026>. 2
- [8] Lili Chen, Kevin Lu, Aravind Rajeswaran, Kimin Lee, Aditya Grover, Michael Laskin, Pieter Abbeel, Aravind Srinivas, and Igor Mordatch. Decision transformer: Reinforcement learning via sequence modeling. In A. Beygelzimer, Y. Dauphin, P. Liang, and J. Wortman Vaughan, editors, *Advances in Neural Information Processing Systems*, 2021. URL <https://openreview.net/forum?id=a7APmM4B9d>. 2
- [9] Zichen Jeff Cui, Hengkai Pan, Aadithya Iyer, Siddhant Haldar, and Lerrel Pinto. Dynamo: In-domain dynamics pretraining for visuo-motor control. In *The Thirty-eighth Annual Conference on Neural Information Processing Systems*, 2024. URL <https://arxiv.org/abs/2409.12192>. 2
- [10] Peter Dayan. Improving generalization for temporal difference learning: The successor representation. *Neural Computation*, 5(4):613–624, 1993. doi: 10.1162/neco.1993.5.4.613. 2, 3
- [11] Scott Emmons, Benjamin Eysenbach, Ilya Kostrikov, and Sergey Levine. Rvs: What is essential for offline RL via supervised learning? In *International Conference on Learning Representations*, 2022. URL <https://openreview.net/forum?id=S874XAIpkR->. 2

[12] Benjamin Eysenbach, Tianjun Zhang, Sergey Levine, and Russ R Salakhutdinov. Contrastive learning as goal-conditioned reinforcement learning. *Advances in Neural Information Processing Systems*, 35:35603–35620, 2022. 3.1, 5

[13] Jesse Farnsworth, Joshua Greaves, Rishabh Agarwal, Charline Le Lan, Ross Goroshin, Pablo Samuel Castro, and Marc G Bellemare. Proto-value networks: Scaling representation learning with auxiliary tasks. In *The Eleventh International Conference on Learning Representations*, 2023. URL <https://openreview.net/forum?id=oGDKSt9JrZi>. 2

[14] Vincent François-Lavet, Yoshua Bengio, Doina Precup, and Joelle Pineau. Combined reinforcement learning via abstract representations. In *Proceedings of the AAAI Conference on Artificial Intelligence*, volume 33, pages 3582–3589, 2019. URL <https://arxiv.org/abs/1809.04506>. 2

[15] Quentin Garrido, Mahmoud Assran, Nicolas Ballas, Adrien Bardes, Laurent Najman, and Yann LeCun. Learning and leveraging world models in visual representation learning, 2024. URL <https://arxiv.org/abs/2403.00504>. 3.1

[16] Carles Gelada, Saurabh Kumar, Jacob Buckman, Ofir Nachum, and Marc G Bellemare. Deepmdp: Learning continuous latent space models for representation learning. In *International conference on machine learning*, pages 2170–2179. PMLR, 2019. URL <https://arxiv.org/abs/1906.02736>. 2, 3.1

[17] Dibya Ghosh, Homer Rich Walke, Karl Pertsch, Kevin Black, Oier Mees, Sudeep Dasari, Joey Hejna, Tobias Kreiman, Charles Xu, Jianlan Luo, You Liang Tan, Lawrence Yunliang Chen, Quan Vuong, Ted Xiao, Pannag R. Sanketi, Dorsa Sadigh, Chelsea Finn, and Sergey Levine. Octo: An open-source generalist robot policy. In *Robotics: Science and Systems*, 2024. URL <https://doi.org/10.15607/RSS.2024.XX.090>. 1

[18] Raj Ghugare, Matthieu Geist, Glen Berseth, and Benjamin Eysenbach. Closing the gap between TD learning and supervised learning - a generalisation point of view. In *The Twelfth International Conference on Learning Representations*, 2024. URL <https://arxiv.org/abs/2401.11237>. 1, 2, 3.2, 3.2

[19] Jean-Bastien Grill, Florian Strub, Florent Altché, Corentin Tallec, Pierre Richemond, Elena Buchatskaya, Carl Doersch, Bernardo Avila Pires, Zhaohan Guo, Mohammad Gheshlaghi Azar, et al. Bootstrap your own latent-a new approach to self-supervised learning. *Advances in neural information processing systems*, 33:21271–21284, 2020. URL <https://arxiv.org/abs/2006.07733>. 1, 3.1, 4.2

[20] Zhaohan Daniel Guo, Bernardo Avila Pires, Bilal Piot, Jean-Bastien Grill, Florent Altché, Remi Munos, and Mohammad Gheshlaghi Azar. Bootstrap latent-predictive representations for multitask reinforcement learning. In Hal Daumé III and Aarti Singh, editors, *Proceedings of the 37th International Conference on Machine Learning*, volume 119 of *Proceedings of Machine Learning Research*, pages 3875–3886. PMLR, 13–18 Jul 2020. URL <https://proceedings.mlr.press/v119/guo20g.html>. 4.1

[21] Nicklas Hansen, Xiaolong Wang, and Hao Su. Temporal difference learning for model predictive control. In *International Conference on Machine Learning (ICML)*, 2022. URL <https://arxiv.org/abs/2203.04955>. 2

[22] Alexander Khazatsky, Karl Pertsch, Suraj Nair, Ashwin Balakrishna, Sudeep Dasari, Siddharth Karamcheti, Soroush Nasiriany, Mohan Kumar Srirama, Lawrence Yunliang Chen, Kirsty Ellis, Peter David Fagan, Joey Hejna, Masha Itkina, Marion Lepert, Yecheng Jason Ma, Patrick Tree Miller, Jimmy Wu, Suneel Belkhale, Shivin Dass, Huy Ha, Arhan Jain, Abraham Lee, Young-woon Lee, Marius Memmel, Sungjae Park, Ilija Radosavovic, Kaiyuan Wang, Albert Zhan, Kevin Black, Cheng Chi, Kyle Beltran Hatch, Shan Lin, Jingpei Lu, Jean Mercat, Abdul Rehman, Pannag R Sanketi, Archit Sharma, Cody Simpson, Quan Vuong, Homer Rich Walke, Blake Wulfe, Ted Xiao, Jonathan Heewon Yang, Arefeh Yavary, Tony Z. Zhao, Christopher Agia, Rohan Baijal, Mateo Guaman Castro, Daphne Chen, Qiuyu Chen, Trinity Chung, Jaimyn Drake, Ethan Paul Foster, Jensen Gao, David Antonio Herrera, Minho Heo, Kyle Hsu, Jiaheng Hu, Donovan Jackson, Charlotte Le, Yunshuang Li, Xinyu Lin, Zehan Ma, Abhiram Maddukuri,

Suvir Mirchandani, Daniel Morton, Tony Khuong Nguyen, Abigail O’Neill, Rosario Scalise, Derick Seale, Victor Son, Stephen Tian, Emi Tran, Andrew E. Wang, Yilin Wu, Annie Xie, Jingyun Yang, Patrick Yin, Yunchu Zhang, Osbert Bastani, Glen Berseth, Jeannette Bohg, Ken Goldberg, Abhinav Gupta, Abhishek Gupta, Dinesh Jayaraman, Joseph J Lim, Jitendra Malik, Roberto Martín-Martín, Subramanian Ramamoorthy, Dorsa Sadigh, Shuran Song, Jiajun Wu, Michael C. Yip, Yuke Zhu, Thomas Kollar, Sergey Levine, and Chelsea Finn. DROID: A large-scale in-the-wild robot manipulation dataset. In *RSS 2024 Workshop: Data Generation for Robotics*, 2024. URL <https://openreview.net/forum?id=M12pTYLNLi>. 1

[23] Khimya Khetarpal, Zhaohan Daniel Guo, Bernardo Avila Pires, Yunhao Tang, Clare Lyle, Mark Rowland, Nicolas Heess, Diana L Borsa, Arthur Guez, and Will Dabney. A unifying framework for action-conditional self-predictive reinforcement learning. In *The 28th International Conference on Artificial Intelligence and Statistics*, 2025. URL <https://arxiv.org/abs/2406.02035>. 1, 2, 3.1, 4.1, D.1, D.1

[24] Moo Jin Kim, Karl Pertsch, Siddharth Karamcheti, Ted Xiao, Ashwin Balakrishna, Suraj Nair, Rafael Rafailov, Ethan P Foster, Pannag R Sanketi, Quan Vuong, Thomas Kollar, Benjamin Burchfiel, Russ Tedrake, Dorsa Sadigh, Sergey Levine, Percy Liang, and Chelsea Finn. OpenVLA: An open-source vision-language-action model. In *8th Annual Conference on Robot Learning*, 2024. URL <https://arxiv.org/abs/2406.09246>. 1

[25] Ilya Kostrikov, Ashvin Nair, and Sergey Levine. Offline reinforcement learning with implicit q-learning. In *International Conference on Learning Representations*, 2022. URL <https://arxiv.org/abs/2110.06169>. 5

[26] Charline Le Lan, Stephen Tu, Adam Oberman, Rishabh Agarwal, and Marc G. Bellemare. On the generalization of representations in reinforcement learning, 2022. URL <https://arxiv.org/abs/2203.00543>. 2

[27] Yann LeCun. A path towards autonomous machine intelligence version, 2022. URL <https://openreview.net/forum?id=BZ5a1r-kVsF>. 3.1

[28] Jaewoo Lee, Sujin Yun, Taeyoung Yun, and Jinkyoo Park. GTA: Generative trajectory augmentation with guidance for offline reinforcement learning. In *The Thirty-eighth Annual Conference on Neural Information Processing Systems*, 2024. URL <https://openreview.net/forum?id=kZpNDbZrzy>. 2

[29] Sergey Levine, Aviral Kumar, George Tucker, and Justin Fu. Offline reinforcement learning: Tutorial, review, and perspectives on open problems, 2020. URL <https://arxiv.org/abs/2005.01643>. 1, 2

[30] Bo Liu, Yihao Feng, Qiang Liu, and Peter Stone. Metric residual network for sample efficient goal-conditioned reinforcement learning. In *Proceedings of the AAAI Conference on Artificial Intelligence*, volume 37, pages 8799–8806, 2023. URL <https://arxiv.org/abs/2208.08133>. 2

[31] Cong Lu, Philip J. Ball, Yee Whye Teh, and Jack Parker-Holder. Synthetic experience replay. In *Thirty-seventh Conference on Neural Information Processing Systems*, 2023. URL <https://openreview.net/forum?id=6jNQ1AY1Uf>. 2

[32] Yunhao Luo, Utkarsh A. Mishra, Yilun Du, and Danfei Xu. Generative trajectory stitching through diffusion composition, 2025. URL <https://arxiv.org/abs/2503.05153>. 2

[33] Arjun Majumdar, Karmesh Yadav, Sergio Arnaud, Yecheng Jason Ma, Claire Chen, Sneha Silwal, Aryan Jain, Vincent-Pierre Berges, Tingfan Wu, Jay Vakil, Pieter Abbeel, Jitendra Malik, Dhruv Batra, Yixin Lin, Oleksandr Maksymets, Aravind Rajeswaran, and Franziska Meier. Where are we in the search for an artificial visual cortex for embodied intelligence? In *Thirty-seventh Conference on Neural Information Processing Systems*, 2023. URL <https://arxiv.org/abs/2303.18240>. 2

[34] Vivek Myers, Chongyi Zheng, Anca Dragan, Sergey Levine, and Benjamin Eysenbach. Learning temporal distances: Contrastive successor features can provide a metric structure for decision-making. In *Forty-first International Conference on Machine Learning*, 2024. URL <https://openreview.net/forum?id=xQiYCmDrjp>. 2

[35] Vivek Myers, Catherine Ji, and Benjamin Eysenbach. Horizon Generalization in Reinforcement Learning. In *International Conference on Learning Representations*, January 2025. URL <https://arxiv.org/pdf/2501.02709.pdf>. 2

[36] Vivek Myers, Bill Chunyuan Zheng, Anca Dragan, Kuan Fang, and Sergey Levine. Temporal representation alignment: Successor features enable emergent compositionality in robot instruction following, 2025. URL <https://arxiv.org/abs/2502.05454>. 1, 2, 4, 5, A.5

[37] Suraj Nair, Aravind Rajeswaran, Vikash Kumar, Chelsea Finn, and Abhi Gupta. R3m: A universal visual representation for robot manipulation. In *Conference on Robot Learning*, 2022. URL <https://arxiv.org/abs/2203.12601>. 2

[38] Tianwei Ni, Benjamin Eysenbach, Erfan Seyedsalehi, Michel Ma, Clement Gehring, Aditya Mahajan, and Pierre-Luc Bacon. Bridging state and history representations: Understanding self-predictive rl. In *The Twelfth International Conference on Learning Representations*, 2024. URL <https://arxiv.org/abs/2401.08898>. 2, 3.1

[39] Abby O'Neill, Abdul Rehman, Abhiram Maddukuri, Abhishek Gupta, Abhishek Padalkar, Abraham Lee, Acorn Pooley, Agrim Gupta, Ajay Mandlekar, Ajinkya Jain, Albert Tung, Alex Bewley, Alex Herzog, Alex Irpan, Alexander Khazatsky, Anant Rai, Anchit Gupta, Andrew Wang, Anikait Singh, Animesh Garg, Aniruddha Kembhavi, Annie Xie, Anthony Brohan, Antonin Raffin, Archit Sharma, Arefeh Yavary, Arhan Jain, Ashwin Balakrishna, Ayzaan Wahid, Ben Burgess-Limerick, Beomjoon Kim, Bernhard Schölkopf, Blake Wulfe, Brian Ichter, Cewu Lu, Charles Xu, Charlotte Le, Chelsea Finn, Chen Wang, Chenfeng Xu, Cheng Chi, Chenguang Huang, Christine Chan, Christopher Agia, Chuer Pan, Chuyuan Fu, Coline Devin, Danfei Xu, Daniel Morton, Danny Driess, Daphne Chen, Deepak Pathak, Dhruv Shah, Dieter Büchler, Dinesh Jayaraman, Dmitry Kalashnikov, Dorsa Sadigh, Edward Johns, Ethan Foster, Fangchen Liu, Federico Ceola, Fei Xia, Feiyu Zhao, Freek Stulp, Gaoyue Zhou, Gaurav S. Sukhatme, Gautam Salhotra, Ge Yan, Gilbert Feng, Giulio Schiavi, Glen Berseth, Gregory Kahn, Guanzhi Wang, Hao Su, Hao-Shu Fang, Haochen Shi, Henghui Bao, Heni Ben Amor, Henrik I Christensen, Hiroki Furuta, Homer Walke, Hongjie Fang, Huy Ha, Igor Mordatch, Ilija Radosavovic, Isabel Leal, Jacky Liang, Jad Abou-Chakra, Jaehyung Kim, Jaimyn Drake, Jan Peters, Jan Schneider, Jasmine Hsu, Jeannette Bohg, Jeffrey Bingham, Jeffrey Wu, Jensen Gao, Jiaheng Hu, Jiajun Wu, Jialin Wu, Jiankai Sun, Jianlan Luo, Jiayuan Gu, Jie Tan, Jihoon Oh, Jimmy Wu, Jingpei Lu, Jingyun Yang, Jitendra Malik, João Silvério, Joey Hejna, Jonathan Booher, Jonathan Tompson, Jonathan Yang, Jordi Salvador, Joseph J. Lim, Junhyek Han, Kaiyuan Wang, Kanishka Rao, Karl Pertsch, Karol Hausman, Keegan Go, Keerthana Gopalakrishnan, Ken Goldberg, Kendra Byrne, Kenneth Oslund, Kento Kawaharazuka, Kevin Black, Kevin Lin, Kevin Zhang, Kiana Ehsani, Kiran Lekkala, Kirsty Ellis, Krishan Rana, Krishnan Srinivasan, Kuan Fang, Kunal Pratap Singh, Kuo-Hao Zeng, Kyle Hatch, Kyle Hsu, Laurent Itti, Lawrence Yunliang Chen, Lerrel Pinto, Li Fei-Fei, Liam Tan, Linxi Jim Fan, Lionel Ott, Lisa Lee, Luca Weihs, Magnum Chen, Marion Lepert, Marius Memmel, Masayoshi Tomizuka, Masha Itkina, Mateo Guaman Castro, Max Spero, Maximilian Du, Michael Ahn, Michael C. Yip, Mingtong Zhang, Mingyu Ding, Minho Heo, Mohan Kumar Srirama, Mohit Sharma, Moo Jin Kim, Naoaki Kanazawa, Nicklas Hansen, Nicolas Heess, Nikhil J Joshi, Niko Suenderhauf, Ning Liu, Norman Di Palo, Nur Muhammad Mahi Shafiullah, Oier Mees, Oliver Kroemer, Osbert Bastani, Pannag R Sanketi, Patrick Tree Miller, Patrick Yin, Paul Wohlhart, Peng Xu, Peter David Fagan, Peter Mitrano, Pierre Sermanet, Pieter Abbeel, Priya Sundaresan, Qiuyu Chen, Quan Vuong, Rafael Rafailov, Ran Tian, Ria Doshi, Roberto Martín-Martín, Rohan Baijal, Rosario Scalise, Rose Hendrix, Roy Lin, Runjia Qian, Ruohan Zhang, Russell Mendonca, Rutav Shah, Ryan Hoque, Ryan Julian, Samuel Bustamante, Sean Kirmani, Sergey Levine, Shan Lin, Sherry Moore, Shikhar Bahl, Shivin Dass, Shubham Sonawani, Shuran Song, Sichun Xu, Siddhant Haldar, Siddharth Karamchetti, Simeon Adebola, Simon Guist, Soroush Nasiriany, Stefan Schaal, Stefan Welker, Stephen Tian, Subramanian Ramamoorthy, Sudeep Dasari, Suneel Belkhale, Sungjae Park, Suraj Nair, Suvir Mirchandani, Takayuki Osa, Tanmay Gupta, Tatsuya Harada, Tatsuya Matsushima, Ted Xiao, Thomas Kollar, Tianhe Yu, Tianli Ding, Todor Davchev, Tony Z. Zhao, Travis Armstrong, Trevor Darrell, Trinity Chung, Vidhi Jain, Vincent Vanhoucke, Wei Zhan, Wenxuan Zhou, Wolfram Burgard, Xi Chen, Xiaolong Wang, Xinghao Zhu, Xinyang Geng, Xiyuan Liu, Xu Liangwei, Xuanlin Li, Yao Lu, Yecheng Jason Ma, Yejin Kim, Yevgen Chebotar, Yifan Zhou, Yifeng Zhu, Yilin Wu, Ying Xu, Yixuan Wang,

Yonatan Bisk, Yoonyoung Cho, Youngwoon Lee, Yuchen Cui, Yue Cao, Yueh-Hua Wu, Yujin Tang, Yuke Zhu, Yunchu Zhang, Yunfan Jiang, Yunshuang Li, Yunzhu Li, Yusuke Iwasawa, Yutaka Matsuo, Zehan Ma, Zhuo Xu, Zichen Jeff Cui, Zichen Zhang, and Zipeng Lin. Open x-embodiment: Robotic learning datasets and rt-x models : Open x-embodiment collaboration0. In *2024 IEEE International Conference on Robotics and Automation (ICRA)*, pages 6892–6903, 2024. doi: 10.1109/ICRA57147.2024.10611477. 1

[40] Seohong Park, Kevin Frans, Benjamin Eysenbach, and Sergey Levine. Ogbench: Benchmarking offline goal-conditioned rl. In *International Conference on Learning Representations (ICLR)*, 2025. URL <https://arxiv.org/abs/2007.05929>. 1, 5, A.5

[41] Alec Radford, Jong Wook Kim, Chris Hallacy, Aditya Ramesh, Gabriel Goh, Sandhini Agarwal, Girish Sastry, Amanda Askell, Pamela Mishkin, Jack Clark, Gretchen Krueger, and Ilya Sutskever. Learning transferable visual models from natural language supervision. In *International Conference on Machine Learning*, 2021. URL <https://arxiv.org/abs/2103.00020>. A.3

[42] Ilija Radosavovic, Tete Xiao, Stephen James, Pieter Abbeel, Jitendra Malik, and Trevor Darrell. Real-world robot learning with masked visual pre-training. In *6th Annual Conference on Robot Learning*, 2022. URL <https://arxiv.org/abs/2203.06173>. 2

[43] Juergen Schmidhuber. Reinforcement learning upside down: Don't predict rewards – just map them to actions, 2020. URL <https://arxiv.org/abs/1912.02875>. 2

[44] Max Schwarzer, Ankesh Anand, Rishab Goel, R. Devon Hjelm, Aaron C. Courville, and Philip Bachman. Data-efficient reinforcement learning with self-predictive representations. In *International Conference on Learning Representations*, 2020. URL <https://arxiv.org/abs/2007.05929>. 1, 2, 3.1, 4.2

[45] Vlad Sobal, Wancong Zhang, Kynghyun Cho, Randall Balestrieri, Tim G. J. Rudner, and Yann LeCun. Learning from reward-free offline data: A case for planning with latent dynamics models, 2025. URL <https://arxiv.org/abs/2502.14819>. 2

[46] Yunhao Tang, Zhaohan Daniel Guo, Pierre H. Richemond, Bernardo Ávila Pires, Yash Chandak, Rémi Munos, Mark Rowland, Mohammad Gheshlaghi Azar, Charline Le Lan, Clare Lyle, András Gyorgy, Shantanu Thakoor, Will Dabney, Bilal Piot, Daniele Calandriello, and M. Valko. Understanding self-predictive learning for reinforcement learning. In *International Conference on Machine Learning*, 2022. URL <https://arxiv.org/abs/2212.03319>. 2, 3.1, 4.1, D.1, D.1, D.1

[47] Ahmed Touati, Jérémie Rapin, and Yann Ollivier. Does zero-shot reinforcement learning exist? In *The Eleventh International Conference on Learning Representations*, 2023. URL [https://openreview.net/forum?id=MYEap\\_0cQI](https://openreview.net/forum?id=MYEap_0cQI). 3.1, 4, A.4, C, D.1

[48] Aaron van den Oord, Yazhe Li, and Oriol Vinyals. Representation learning with contrastive predictive coding, 2019. URL <https://arxiv.org/abs/1807.03748>. 1, 3.1

[49] Claas A. Voelcker, Tyler Kastner, Igor Gilitschenski, and Amir-massoud Farahmand. When does self-prediction help? understanding auxiliary tasks in reinforcement learning. *Reinforcement Learning Conference*, August 2024. URL <https://arxiv.org/abs/2406.17718>. 2

[50] Tongzhou Wang and Phillip Isola. Improved representation of asymmetrical distances with interval quasimetric embeddings. In *NeurIPS 2022 Workshop on Symmetry and Geometry in Neural Representations*, 2022. URL <https://arxiv.org/abs/2211.15120>. 2

[51] Tongzhou Wang, Antonio Torralba, Phillip Isola, and Amy Zhang. Optimal goal-reaching reinforcement learning via quasimetric learning. In *International Conference on Machine Learning*. PMLR, 2023. URL <https://arxiv.org/abs/2304.01203>. 2, 5

[52] Taku Yamagata, Ahmed Khalil, and Raúl Santos-Rodríguez. Q-learning decision transformer: leveraging dynamic programming for conditional sequence modelling in offline rl. In *Proceedings of the 40th International Conference on Machine Learning*, ICML'23. JMLR.org, 2023. 1, 2

- [53] Weirui Ye, Shaohuai Liu, Thanard Kurutach, Pieter Abbeel, and Yang Gao. Mastering atari games with limited data. *Advances in neural information processing systems*, 34:25476–25488, 2021. URL <https://arxiv.org/abs/2111.00210>. 2
- [54] Zhaoyi Zhou, Chunling Zhu, Runlong Zhou, Qiwen Cui, Abhishek Gupta, and Simon Shaolei Du. Free from bellman completeness: Trajectory stitching via model-based return-conditioned supervised learning. In *The Twelfth International Conference on Learning Representations*, 2024. URL <https://arxiv.org/abs/2310.19308>. 2

## A Experimental Setup

Table 3: Hyperparameters for BYOL- $\gamma$

Hyperparameter	Shared	
actor head	MLP (512,512,512)	
representation encoder ( $\phi$ )	MLP (64,64,64)	
predictor ( $\psi$ )	MLP (64,64,64)	
encoder ensemble	2	
learning rate	$3 \times 10^{-4}$	
optimizer	Adam	
	Non-visual	Visual
Gradient steps	1000k	500k
Batch size	1024	256
$\tau$ (EMA)	1.0	0.99
$\gamma$	0.99	{0.66, 0.99}
$\alpha$ (alignment)	{1,6,40,100}	{1,6,10,20}
additional encoder	n/a	impala_small
encoder output dimension	$ s $	64

### A.1 Implementation Details

In this section we provide more training details for BYOL- $\gamma$ , and representation learning baselines. We match the training details of OGBench, including gradient steps, batch size, learning rate.

**Network Architecture.** We follow the same network architecture setup as TRA, where we utilize MLP-based encoders, and action head. For the output dimension of the encoder, we use the state dimension for non-visual experiments, and 64 for visual experiments. For the predictor  $\psi$ , we utilize an MLP of the same architecture as the encoder. For image-based tasks, there is an additional CNN, which then passes output to the MLP encoder.

**Representation Ensemble.** We follow the setup of TRA which utilizes representation ensembling, such that two copies of the encoder  $\phi_1, \phi_2$  are in parallel. We also have two distinct predictors  $\psi_1, \psi_2$  for each ensemble. As input to the policy head, we average the representations,  $\bar{z} = \frac{\phi_1(s_t) + \phi_2(s_t)}{2}$ . Each representation is trained independently for the BYOL loss, but the BC loss differentiates through both  $\phi$ s.

**Alignment.** We find that the choice of weight of the auxiliary loss for the representation learning objective is sensitive to both the robot embodiment and the environment size. For comparison, we perform a hyperparameter search over four alignment values for BYOL- $\gamma$ , TRA, and FB, and then report the best value for each environment in Table 1.

**Discount.** For sampling the next-state, we utilize a discount factor of  $\gamma = 0.99$  for all non-visual environments. For visual environments, we perform a hyperparameter search over {0.66, 0.99}, however all representation learning methods performed better at  $\gamma = 0.66$ .

### A.2 BYOL- $\gamma$

**Target network.** For BYOL, we find that exponential moving average (EMA) target networks for the encoder  $\phi$  are not necessary for non-visual environments ( $\tau = 1$ ), but for visual environments, we find that a fast target stabilizes training ( $\tau = 0.99$ ):

$$\phi_{\text{target}} = \tau \phi_{\text{online}} + (1 - \tau) \phi_{\text{target}}$$

### A.3 TRA

In practice, TRA uses a symmetric version [41] of the InfoNCE objective discussed in Equation 3. We write this in batch form,  $\mathcal{B} = \{(s_i, s_{+,i})\}_{i=1}^{|\mathcal{B}|}$  rather than in expectation:

$$\mathcal{L}_{\text{TRA}} = \mathbb{E}_{\mathcal{B}} \left[ -\frac{1}{B} \sum_{i=1}^{|\mathcal{B}|} \log \frac{e^{f(\psi(s_i), \phi(s_{+,i}))}}{\sum_{j=1}^{|\mathcal{B}|} e^{f(\psi(s_i), \phi(s_{+,j}))}} - \frac{1}{B} \sum_{i=1}^{|\mathcal{B}|} \log \frac{e^{f(\psi(s_i), \phi(s_{+,i}))}}{\sum_{j=1}^{|\mathcal{B}|} e^{f(\psi(s_j), \phi(s_{+,i}))}} \right] \quad (16)$$

Additionally, TRA minimizes the squared norm of representations  $\min_{\phi, \psi} \lambda \mathbb{E}_s \left[ \frac{\|\phi(s)\|^2}{d} + \frac{\|\psi(s)\|^2}{d} \right]$  with  $\lambda = 10^{-6}$ . For TRA, we search over  $\alpha = \{10, 40, 60, 100\}$ .

### A.4 FB

Prior work which trains FB for zero-shot policy optimization [47] typically normalizes  $\phi$  with an additional loss term so that  $\mathbb{E}[\phi\phi^T] \approx I_d$ . However, we found that adding this loss term was not beneficial to performance in our setting and hence do not include it.

FB uses an EMA target network as described in A.2 with  $\tau = 0.005$ . For FB, we search over  $\alpha = \{0.01, 0.05, 0.001, 0.005\}$ .

### A.5 Code.

We utilize the OGBench [40] codebase and benchmark, and its extensions in the TRA codebase [36] for equal comparison.

### A.6 Compute Requirements

We perform all experiments utilizing single GPUs, predominately NVIDIA RTXA8000 and L40S. We utilize 6 CPU cores, 24G of RAM for non-visual environments, and 64G for visual experiments. Experiments take 2 to 4 hours for non-visual and 6 to 12 hours for visual environments.

## B Ablations.

### B.1 Action-conditioning

In this section, we ablate the component of performing action-conditioning for the predictor  $\psi(s_t)$  vs  $\psi(s_t, a_t)$  for TRA and FB. We consider a similar comparison for BYOL- $\gamma$  in Table 2. For this comparison, when we perform action-conditioning, we utilize a policy representation  $\pi(s = \phi(s), g = \phi(g))$ , and otherwise  $\pi(s = \psi(s), g = \phi(g))$ . We find that results can be environment specific. On average, results are not improved for TRA, but we find an improvement for FB, hence in our main Table 1 we include the action-conditioned results for FB and the action-free results for TRA.

Dataset	TRA	TRA <sup>a</sup>	FB	FB <sup>a</sup>
antmaze-medium-stitch	54 ± 6	57 ± 12	<b>64 ± 10</b>	<b>64 ± 6</b>
antmaze-large-stitch	11 ± 8	7 ± 7	17 ± 6	<b>23 ± 4</b>
humanoidmaze-medium-stitch	<b>45 ± 8</b>	<b>45 ± 5</b>	36 ± 3	42 ± 4
humanoidmaze-large-stitch	5 ± 4	9 ± 4	6 ± 2	<b>11 ± 3</b>
antsoccer-arena-stitch	14 ± 4	<b>25 ± 8</b>	17 ± 5	22 ± 10
visual-antmaze-medium-stitch	<b>52 ± 3</b>	33 ± 4	47 ± 5	<b>49 ± 2</b>
visual-antmaze-large-stitch	17 ± 1	22 ± 5	<b>28 ± 3</b>	<b>29 ± 2</b>
visual-scene-play	16 ± 3	<b>18 ± 2</b>	12 ± 2	14 ± 1
average	27	27	28	32

Table 4: **Action-conditioning ablations.** We ablate the choice to condition on the first action for predictor  $\psi$  for TRA and FB over 10 seeds for non-visual and 4 seeds for visual environments.

## C CL to FB

Here, illustrate that connection between CL and FB, showing that in the limit an n-step version of FB becomes similar to CL.

We can rewrite Equation (3) to see the connection between FB (TD) and CL (MC). Under assumptions that  $\phi, \psi$  are centered ( $\mathbb{E}[\phi] = \mathbb{E}[\psi] = 0$ ), and unit normalized  $\|\phi\|_2, \|\psi\|_2 = 1$ , if we apply a second-order Taylor expansion to the denominator of the CL loss [47] we have:

$$\text{CL}_{\text{InfoNCE}} \approx \frac{1}{2} \mathbb{E}_{s \sim p_0(s), s' \sim p_0(s')} [(\psi(s)^T \phi(s'))^2] - 2 \mathbb{E}_{\substack{k \sim \text{geom}(1-\gamma) \\ s_t \sim p_0, s_{t+k} \sim p^\pi(s_{t+k}|s_t)}} [\psi(s_t)^T \phi(s_{t+k})] \quad (17)$$

Next, we can consider an n-step variant of the FB loss [2] which we refer to as  $\text{FB}(n)$ :

$$\min_{\phi, \psi} \mathbb{E}_{\substack{s_t \sim p_0 \\ s' \sim p_0}} [(\psi(s_t)^T \phi(s'))^2 - \gamma^n \bar{\psi}(s_{t+n})^T \bar{\phi}(s'))^2] - 2 \sum_{i=1}^n \mathbb{E}_{\substack{s_t \sim p_0, s_{t+i} \sim p^\pi \\ s_{t+i} \sim p^\pi(s_{t+i}|s_0)}} [\gamma^i \psi(s_t)^T \phi(s_{t+i})] \quad (18)$$

We can make the full connection to CL with infinite horizon  $n$ :

$$\text{FB}(n) = \mathbb{E}_{\substack{s_t \sim p_0 \\ s' \sim p_0}} [(\psi(s_t)^T \phi(s'))^2] - 2 \sum_{i=1}^n \mathbb{E}_{\substack{s_t \sim p_0 \\ s_{t+i} \sim p^\pi(s_{t+i}|s_0)}} [\gamma^i \psi(s_t)^T \phi(s_{t+i})] \quad (19)$$

$$= \mathbb{E}_{\substack{s_t \sim p_0 \\ s' \sim p_0}} [(\psi(s_t)^T \phi(s'))^2] - \frac{2\gamma}{(1-\gamma)} \sum_{i=1}^n \mathbb{E}_{\substack{s_t \sim p_0 \\ s_{t+i} \sim p^\pi(s_{t+i}|s_0)}} [(1-\gamma)\gamma^{i-1} \psi(s_t)^T \phi(s_{t+i})] \quad (20)$$

$$= \mathbb{E}_{\substack{s_t \sim p_0 \\ s' \sim p_0}} [(\psi(s_t)^T \phi(s'))^2] - \frac{2\gamma}{(1-\gamma)} \mathbb{E}_{\substack{k \sim \text{geom}(1-\gamma) \\ s_t \sim p_0, s_{t+k} \sim p^\pi(s_{t+k}|s_t)}} [\psi(s_t)^T \phi(s_{t+k})] \quad (21)$$

Thus, we can see that in the infinite horizon form of  $\text{FB}(n)$ , it is related to the form of  $\text{CL}_{\text{InfoNCE}}$  in (3), but with the positive contrastive term weighted by factor  $\frac{\gamma}{1-\gamma}$ .

## D Finite MDP

### D.1 BYOL

**BYOL as an Ordinary Differential Equation (ODE)** In finite MDPs, we can characterize the BYOL objective which gives intuition about what information is captured in  $\phi, \psi$ , and conditions that may be useful for stability [46, 23]. Consider a finite MDP with transition  $P^\pi$ , linear d-dimensional encoder  $\Phi \in \mathbb{R}^{|S| \times d}$ , and linear action-free latent-dynamics  $\Psi \in \mathbb{R}^{d \times d}$ . In a finite MDP, Equation (4) becomes:

$$\min_{\Phi, \Psi} \text{BYOL}(\Phi, \Psi) := \min_{\Phi, \Psi} \mathbb{E}_{s_t \sim p(s), s_{t+1} \sim P^\pi} [\|\psi^T \Phi^T s_t - \bar{\Phi}^T s_{t+1}\|_2^2] \quad (22)$$

A property to prevent this objective from collapsing is that  $\Psi$  is updated more quickly than  $\Phi$ . In practice, this is commonly realized as the dynamics are generally a smaller network than the encoder. This system can be analyzed in an ideal setup, where we first find the optimal  $\Psi$ , each time before taking a gradient step for  $\Phi$ , which leads to the ODE for representations  $\Phi$  [46]:

$$\Psi^* \in \arg \min_{\Psi} \text{BYOL}(\Phi, \Psi), \quad \dot{\Phi} = -\nabla_{\Phi} \text{BYOL}(\Phi, \Psi)|_{\Psi=\Psi^*} \quad (23)$$

We are able to analyze this ODE with the following assumptions [46]:

**Assumption D.1** (Orthogonal initialization).  $\Phi^\top \Phi = I$

**Assumption D.2** (Uniform state distribution).  $p_0(s) = \frac{1}{|S|}$

**Assumption D.3** (Symmetric dynamics).  $P^\pi = (P^\pi)^\top$

Under these three assumptions, Khetarpal et al. [23] prove that the BYOL ODE is equivalent to monotonically minimizing the surrogate objective:

$$\min_{\Psi} \|P^\pi - \Phi\Psi\Phi^T\|_F + C \quad (24)$$

Where  $\|\cdot\|_F$  is the Frobenius matrix norm. Thus, we can understand that the BYOL objective as learning a d-rank decomposition of the underlying dynamics  $P^\pi$ . Additionally, the top  $d$  eigenvectors of  $P^\pi$  match those of  $(I - \gamma P^\pi)^{-1} = M^\pi$  Chandak et al. [6]. However, we will highlight that there are key differences when *learning* a low-rank decomposition between  $P^\pi$  and  $M^\pi$ . This is described by [47], where we can consider that in a real-world problem with underlying continuous-time dynamics, actions have little effect, and  $P^\pi$  is close to the identity, e.g. close to full-rank. However,  $M^\pi$ , which takes powers of  $P_\pi^t$ , has a “sharpening effect” on the difference between eigenvalues, which gives a clearer learning signal. This is intuitive on a real-world problem like robotics, even with discrete-time dynamics, where  $s_{t+1} \approx s_t$ , but we have larger differences between  $s_t$  and  $s_{t+k}$ .

## D.2 BYOL- $\gamma$

**In the finite MDP**, we now verify theorem 4.1, where BYOL- $\gamma$  approximates the successor representation with matrix decomposition  $\tilde{M}^\pi \approx \Phi\Psi\Phi^T$ .

We consider the same objective (22), where we need to update the expectation of the sampling distribution:

$$\min_{\Phi, \Psi} \text{BYOL-}\gamma(\Phi, \Psi) := \min_{\Phi, \Psi} \mathbb{E}_{s_t \sim p(s), s_+ \sim \tilde{M}^\pi, [\|\psi^T \Phi^T s_t - \bar{\Phi}^T s_+\|_2^2]} \quad (25)$$

Assuming that this objective is optimized under the ODE (23). We have that our objective monotonically minimizes:

$$\min_{\Psi} \|\tilde{M}^\pi - \Phi\Psi\Phi^T\|_F + C \quad (26)$$

This directly translates as we can consider  $\tilde{M}^\pi = P^\pi$  as simply a valid transition matrix for a new, temporally abstract, version of the original MDP. We maintain the original assumptions D.1, D.2, and D.3. We do not need an additional assumption for  $\tilde{M}^\pi$ , as assumption D.3 for symmetric  $P^\pi$  implies a symmetric  $\tilde{M}^\pi = (1 - \gamma) \sum_{t \geq 0} \gamma^t P_\pi^t$ .

Under this setup, we also have that  $\Psi\Phi \in \mathbb{R}^{n \times d}$  relates to the successor feature matrix, where each row  $(\Psi\Phi)_i$  contains the vector  $(1 - \gamma)\psi^\pi(s_i)$ :

$$(1 - \gamma)\psi^\pi(s_i) = \sum_j \tilde{M}^\pi(s_i, s_j)\phi(s_j) \quad (27)$$

$$= (\tilde{M}^\pi\Phi)_i \quad (28)$$

$$\approx (\Phi\Psi\Phi^T\Phi)_i \quad (29)$$

$$= (\Phi\Psi)_i \quad (30)$$

In other words, in the restricted finite MDP, where we minimize (26), we are simultaneously learning successor features  $\psi^\pi \approx \Psi\Phi$  and basis features  $\Phi$ .

## E Additional Results for Horizon Generalization

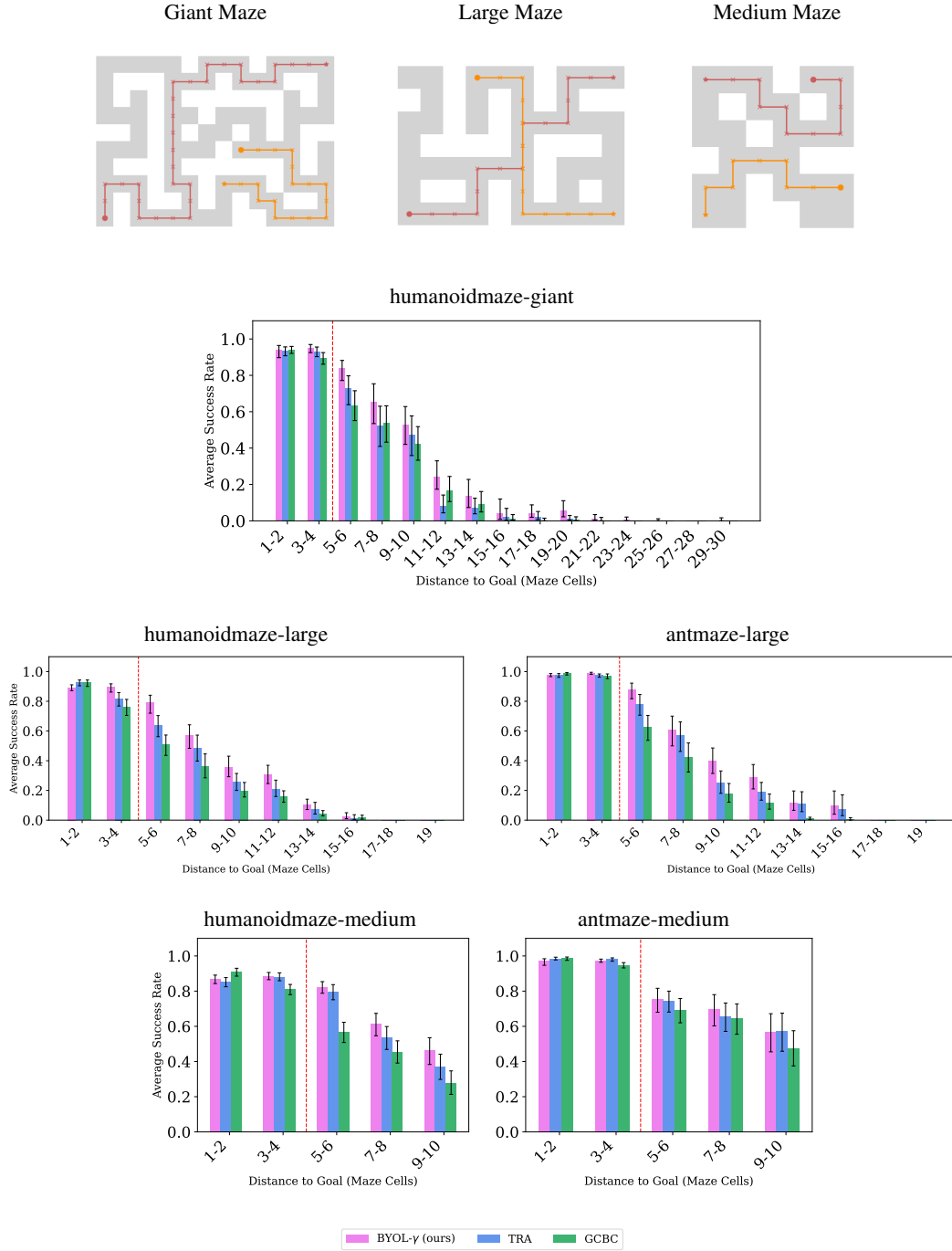


**Figure 4: Evaluating Generalization with Increasing Horizons:** The distances to the right of the red dotted line require combinatorial generalization. The maze maps show examples of how intermediate goals are selected along the optimal path.

We include additional results matching the setup in Section 5.3, for antmaze-medium, and {humanoidmaze}-medium, large, giant} in Figure 4. We can observe that BYOL- $\gamma$  leads in performance as the distance between the start and goal grows when compared to other methods.